行政院國家科學委員會補助專題研究計畫成果報告

※※※※※※※※※※※※※※※※※※※※※※※※※

※ 核反應器縱向裂紋之彈塑性分析 ※

※ Elastic-Plastic Analysis of Reactor ※

※ Vessel Longitudinal Flaws ※

※※※※※※※※※※※※※※※※※※※※※※※※※

計畫類別：V 個別型計畫 □整合型計畫

計畫編號：NSC92－2212－E－216－010

執行期間：92 年 8 月 1 日至 93 年 7 月 31 日

計畫主持人：楊立杰

本成果報告包括以下應繳交之附件：

□赴國外出差或研習心得報告一份

□赴大陸地區出差或研習心得報告一份

□出席國際學術會議心得報告及發表之論文各一份

□國際合作研究計畫國外研究報告書一份

執行單位：中華大學應用數學所

中 華 民 國 93 年 10 月 3 日

行政院國家科學委員會專題研究計畫成果報告
國科會專題研究計畫成果報告撰寫格式說明
Preparation of NSC Project Reports

計畫編號：NSC 92-2212-E-216-010
執行期限：92 年 8 月 1 日至 93 年 7 月 31 日
主持人：楊立杰　中華大學應用數學所

一、中文摘要

本計畫將藉彈塑性邊界元素分析，決定由 EPRI 所提出的 J 估計法中的修正因子。亦將由一個核反應爐表面上的半橢圓形裂紋，來分析核反應器的完整性，而這個最大深度為壁厚四分之一的裂紋是被 ASME Code Section III, Appendix G 用來作為參考的，其結果在 1982 年由 deLorenzi 發表，而 Bloom 又由此推導出了此種裂紋的修正函數。本計畫將應用邊界元素法來驗證 deLorenzi 結果的正確性，並將擴展到另外三種不同深度的裂紋。

彈塑性分析將依據先前的論文 Young [1]而被應用在這核反應爐腹帶區的四種不同深度的假定表面裂紋上，此四種內表面半橢圓裂紋的長寬比均為 6:1，且穿透壁厚的深度分別為 1/8, 1/4, 3/8, 1/2 的壁厚。二維及三維邊界元素分析將藉著塑性變形定理而執行，四種裂紋的 J 積分值亦將擴展三維邊界元素法的資料庫。

關鍵詞：腹帶區

Abstract

For elastic-plastic fracture mechanics analysis, the J-estimation method introduced by the Electric Power Research Institute (EPRI) fracture handbook, An Engineering Approach for Elastic-Plastic Fracture Analysis, will be used extensively. This estimation method required a calibration function in predicting the plastic contribution term of J. This calibration function will be determined from an elastic-plastic boundary element analysis of a structure of interest with a crack.

A longitudinal semi-elliptical surface flaw in a reactor vessel will be used in analyzing reactor vessel integrity since this flaw, with a maximum depth of one fourth of the vessel thickness, is used as a reference flaw in the ASME Code Section III, Appendix G. Results published by deLorenzi in 1982. Later, Bloom derived a calibration function for the flaw from deLorenzi's work.

This research is intended to independently verify deLorenzi's work, also using deformation plasticity, but with a different computer program. Furthermore, the present analysis will extend deLorzenzi's work by including three additional flaw depths.

Elastic-plastic analysis will be used to study four postulated longitudinal surface flaws in the beltline region of a pressurized water reactor pressure vessel based on the previous paper of Young [1]. The flaws are 6:1 semi-elliptical inside surface flaws with through-wall penetrations equal to one eight, one quarter, three eights, and one half of the vessel thickness. Two- and three-dimensional analyses will be performed utilizing deformation theory plasticity as implemented in the boundary element program. The J-integral values present for the four surfaces flaws will be intended to extend the database of three-dimensional boundary element results necessary for such flaw evaluation techniques as the failure assessment diagram approach.

Keywords: Beltline Region

二、緣由與目的

The ASME Boiler and Pressure Vessel Code requires that flaws in pressure vessels of pressured water reactors (PWRs), whether postulated at the design stage [2] or detected during in-service inspections [3], be subjected to structural evaluation by fracture mechanics methods. The ASME Code flaw evaluation methods, based on the principles of linear elastic fracture mechanics, are adequate for non-ductile fracture, but they are overly conservative at temperatures where the vessel materials exhibit ductile behavior. Nonlinear fracture mechanics techniques have been used to take into account the beneficial aspects of plastic deformations at the crack tip that serve to increase the tolerance of reactor vessel materials to the presence of a flaw. These effects are most pronounced at the higher pressure-loadings characteristic of certain postulated accident conditions in the nuclear industry. Using finite element analysis, deLorenzi [4] showed that the ASME postulated 1/4 T surface flaw should be treated as a three-dimensional elastic-plastic problem at high pressure loadings.

Elastic-plastic estimation procedures are well documented by Kumar et al. [5] for the cases of infinitely long axial flaws and axisymmetric circumferential flaw in a cylinder. The simplicity of the procedures, which have been shown to be effective over a wide range of pressure loadings, is due to a separation of the elastic-plastic problem into "effective elastic" and "factored fully plastic" solutions. Factors,

termed h_1 functions, are used to ratio fully plastic solutions according to the concepts of proportional loading. These h_1 functions vary with the depth to thickness ratio, the thickness to vessel radius ratio, and the exponent, n, in Ramberg-Osgood power hardening representations of deformation plasticity material behavior. Bloom [6] used deLorenzi's results to calibrate an extended h_1 function, with an added dependency on the crack depth to length ratio, for longitudinal, semi-elliptical, inside-surface flaw in pressurized cylinders.

The postulated two-dimensional ASME reference flaws are located in a longitudinal plane at the inside surface of a typical PWR. The shape of the semi-elliptical crack front, shown in Fig. 1, is

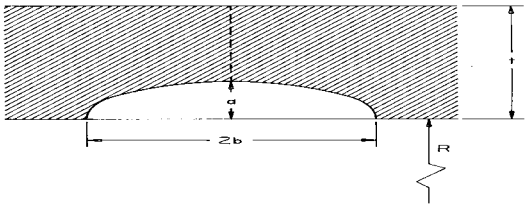

Fig. 1 *Semi-elliptical flaw nomenclature*

characterized by depth, a, and length, 2b, and the pressure vessel, by wall thickness, t, and inside radius, R. The geometries considered here are a constant crack aspect ratio, 2b/a=6, a constant inside radius to wall thickness ratio for the vessel, R/t=10, and varying crack depths extending one eight, one quarter, three eights, and one half of the way through the wall. These crack depths are 1/8 T, 1/4 T, 3/8 T and 1/2 T, respectively.

三、研究報告應含的內容

Three-Dimensional Elastic Result

Elastic-analyses were performed as a preliminary step to check out the three-dimensional semielliptical flaw models. Stress-intensity factors, *K*, were calculated from the *J*-integrals, although the expression for *K* is only rigorously valid for plane strain conditions. At the maximum flaw depth, however, these stress-intensity factors are representative of the actual values since near plane strain conditions exist at that location. To show the variation of *K* along the assumption of plane strain conditions clearly breaks down at the inside surface of the vessel. The variation of the stress-intensity factors along the crack front is shown in Fig. 2 for all four

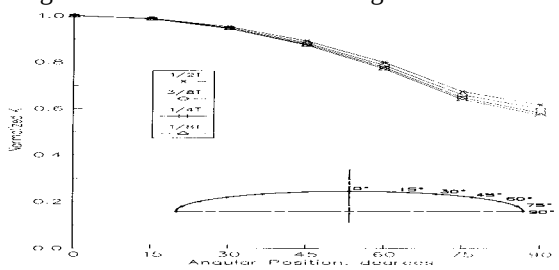

Fig. 2 *J-integral versus internal pressure for semielliptical surface flaws — three-dimensional nonlinear analysis.*

flaw sizes, where the stress-intensity factors have been normalized with respect to the value at the center, or 0°, position. These stress-intensity factors were calculated by linear analysis for an arbitrary of 13.79 MPa (2000 psi) applied to the inside surface of the vessel and the crack face. Figure 2 reveals the consistency of the variation of *K* along the crack front for all four flaw sizes. It is seen from Fig. 2 that, for all flaw sizes, *K* decreases from its maximum value at the center of the crack to about 60% of that value at the surface, and tends to level off at the 75° location. It is noted from an inspection of the angular positions in the inset of Fig. 2 that this leveling off of *K* near the free surface actually occurs over a very small region of the crack front.

Additional results from the three-dimensional linear analyses are presented in Fig. 3, where the *J*-integral at the center of the crack is plotted against pressure for the four flaw sizes. The linear results were

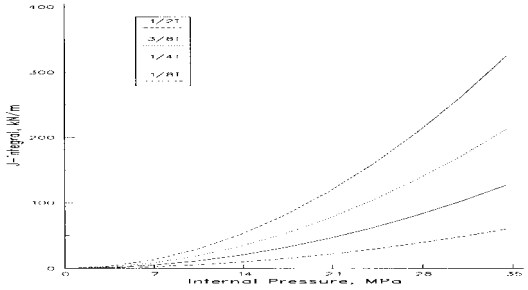

Fig. 3 *J-integral versus internal pressure for semielliptical surface flaws — three-dimensional nonlinear analysis.*

obtained by loading the models with pressure on the inside surface and the crack face, and varying the pressure from 3.447 MPa (500 psi) to 34.37 MPa (5000 psi) with a 3.447 MPa (500 psi) increase in pressure at each load step.

Three-Dimensional Elastic-Plastic Result

Nonlinera analysis was performed on the three-dimensional semielliptical flaw models using the same deformation plasticity, true stress/strain, large displacement approach used for the two-dimensional nonlinear analyses. Pressure, again applied to the inside surface and the crack face, was performed from 0 to 34.47 MPa (5000 psi), and iterative solutions were obtained at each 3.447 MPa (500 psi) increment in load. The variation of the maximum, or center-of-the-crack, *J*-integral with pressure is shown in Fig. 4 for all four flaws suzes.

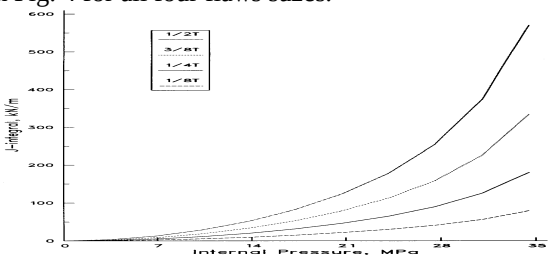

Fig. 4 *J-integral versus internal pressure for semielliptical surface flaws — three-dimensional nonlinear analysis.*

A typical variation of the normalized *J*-integral along the crack front is shown in Fig. 5 for the 1/4*T*

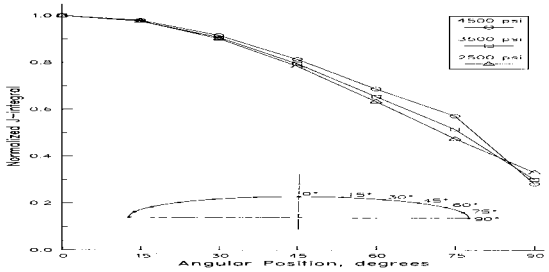

Fig. 5 *Variation of the normailized J-integral along the crack front at three load levels for the 1/4 T flaw.*

flaw size, for pressure-loadings of 17. 24, 24.13, and 31.03 MPa (2500, 3500, and 4500 psi). The 17.24 MPa (2500 psi) pressure level corresponds to the design pressure, and the other two pressure levels chosen to study the influence of plasticity at higher loads. Again, the *J*-integral are normalized with respect to the maximum value at the center. It is seen from Fig. 5 that the curves all tend to peak at the crack centers, and fall off to values less than one half the peak values towards the free surface. This falling off is especially rapid over the 15° of crack front immediately adjacent to the free surface, and appears to be greater at the higher pressure levels. It is suspected that the mesh refinement may not be of sufficient detail along the crack front in the vicinity of the free surface to capture accurate measures of the *J*-integral in this region, and thus the *J*-integral probably do not fall off near the free surface as much as indicated by the curve.

It is informative to compare the three-dimensional nonlinear results with those from the two-dimensional plane strain and linear three-dimensional analyses. The center-of the crack *J*-integral is plotted as a function of pressure for the three solution methods in Fig. 6 for

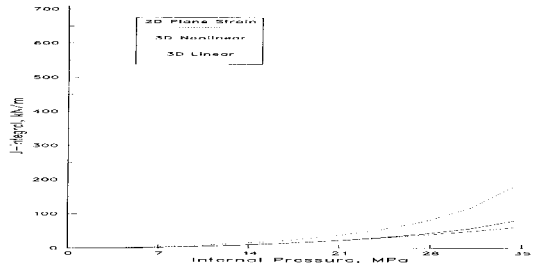

Fig. 6 *J-integral versus pressure for three solution methods—1/8T flaw size.*

the 1/8*T* flaw. Similar curves are presented in Figs. 7 through 9 for the 1/4*T*, 3/8*T*, and 1/2*T* flaws, respectively. These Figures all show a consistent trend, in that the plane strain solutions are extremely conservative, even at low pressure levels, with the degree of conservatism increasing for the large flaw sizes. The three-dimensional linear solutions, on the other hand, track the three-dimensional nonlinear solutions very well up to about the design pressure, or 17.24 MPa (2500 psi), beyond which they become

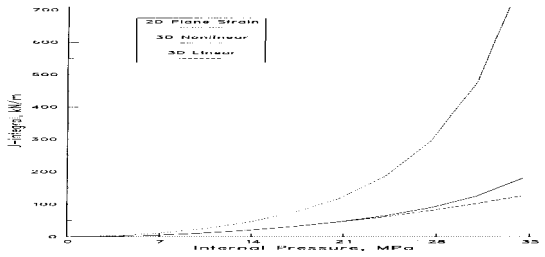

Fig. 7 *J-integral versus pressure for three solution methods—1/4T flaw size.*

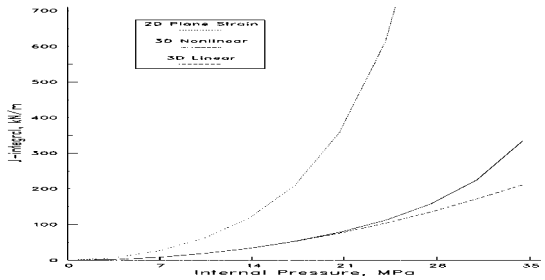

Fig. 8 *J-integral versus pressure for three solution methods—3/8T flaw size.*

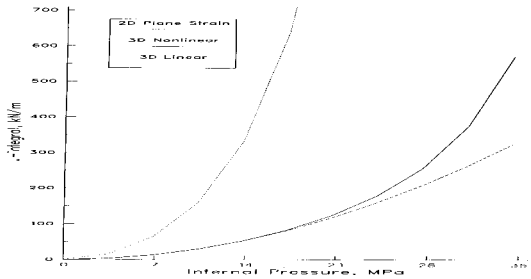

Fig. 9 *J-integral versus pressure for three solution methods—1/2T flaw size.*

increasingly nonconservative. The break point between the linear and nonlinear three-dimensional solutions variesversely with flaw size (Table 1). For the 1/8*T* flaw, the linear and nonlinear solutions begin to diverge at about 24.13 MPa (3500 psi), but for the 1/2*T* flaw, this divergence occurs at only about 13.79 MPa (2000 psi).

Flaw Size	Break-Point Pressure
1/8*T*	24.13 MPa (3500 psi)
1/4*T*	20.68 MPa (3000 psi)
3/8*T*	17.24 MPa (2500 psi)
1/2*T*	13.79 MPa (2000 psi)

Table 1 *Three-dimensional linear/nonlinear break-point pressures*

Elastic-plastic boundary element analysis has been performed to study longitudinally oriented, semielliptical, inside surface flaws in a typical PWR pressure vessel. The depths of the flaws were one eighth, one quarter, three eighths, and one half of the vessel wall thickness, and each had a 6:1 length to depth ratio up to 34.47 MPa (5000 psi), or about twice the design pressure. Results showed that *J*-integrals computed from two-dimensional nonlinear analysis are extremely conservative at all pressure levels.

Three-dimensional linear analysis was shown to produce accurate results for loadings up to about 17.24 MPa (2500 psi), depending on flaw size. At higher pressure-loadings, three-dimensional linear analysis proved to be nonconservative.

Based on the results of this study, it is clear that two-dimensional analysis should only be used for reactor vessel flaw analysis when its inherent conservatism can be accommodated by design conditions, and not when an accurate measure of structural response is required. Different restrictions apply to the use of three-dimensional linear analysis. This method should not be used above the design pressure, where it results in nonconservative values for the *J*-integral. Accurate results for loadings up to about twice the design pressure can only be achieved by three-dimensional nonlinear analysis. Indeed, the three-dimensional results generated by this study can be used to develop the h_1 functions required for flaw evaluations by the elastic-plastic estimation scheme proposed by Kumar et al. [5].

四、參考文獻

[1] Young, Lih-jier, "A Fracture Mechanics Analysis of the PWR Nuclear Power Plant Reactor Pressure Vessel Beltline Weld", J. of Nuclear Materials, 288, 2001, 197-201

[2] ASME Boiler and Pressure Vessel Code, Section III, Appendix G, The American Society of Mechanical Engineers, New York, 1986.

[3] ASME Boiler and Pressure Vessel Code, Section XI, The American Society of Mechanical Engineers, New York, 1986.

[4] deLorenzi, H.G., “Elastic-Plastic Analysis of the Maximum Postulated Flaw in the Beltline Region of a Reactor Vessel,” ASME Journal of Pressure Vessel Technology, Vol. 104, Nov. 1982, pp. 278-286.

[5] Kumar, V., German, M.D., and Shih, C.F., “Elastic-Plastic and Fully Analysis of Crack Initiation, Stable Growth, and Instability in Flawed Cylinders,” Elastic-Plastic Fracture, Second Symposium, Vol. I: Inelastic Crack Analysis, ASTM STP 803, C.F. Shih and J.P. Gudas, Eds., American Society for Testing and Materials, Philadelphia, 1983, pp. 306-353.

[6] Bloom, J.M., ”Extension of the Failure Assessment Diagram Approach — Semi-Elliptical Flaw in pressurized Cylinder, “ASME Journal of Pressure Vessel Technology, Vol. 107, Feb. 1985, pp. 278-286.

[7] Young, Lih-jier, 2002, “An Analysis of a Fracture Specimen for Rough Crack in Shear”, Int’l J. of Fracture,

[8] Hutchinson, J.W., “Singular Behavior at the End of a Tensile Crack in a Hardening Material,” Journal of the Mechanics and Physics of Solids, Vol. 16, No. 1, Jan. 1968, pp. 13-31.

[9] Rice, J.R., and Rosengren, G.F., “Plane Strain Deformation Near a Crack Tip in a Power Law Hardening Material,” Journal of the Mechanics and Physics of Solids, Vol. 16, No. 1, Jan. 1968, pp. 1-12.

[10] Hutchinson, J.W. and Paris, P.C., “Stability Analysis of J-Controlled Crack Growth,” Elastic-Plastic Fracture, ASTM STP 668, J.D. Landes, J.A. Begley, and G.A. Clarke, Eds., American Society for Testing and Materials, Philadelphia, 1979, pp. 37-64.

[11] Young, Lih-jier, and Yeong-pei Tsai, "A Boundary Element Application for Mixed Mode loading Idealized Sawtooth Fracture Surface", Int’l J. of Solids and Structures, 36, 1999, pp. 3239-3252.

[12] Young, Lih-jier, "Lifetime Evaluation of Cracked Shaft Sleeve of Reactor Coolant Pump under Thermal Striping", Int'l J. of Solids and Structures, 38, 2001, 8345-8358.